Science of the Total Environment 801 (2021) 149343

Contents lists available at ScienceDirect

Science of the Total Environment

journal homepage: www.elsevier.com/locate/scitotenv

Modelling the sorption behaviour of perfluoroalkyl carboxylates and perfluoroalkane sulfonates in soils

Joel Fabregat-Palau, Miquel Vidal, Anna Rigol *

Department of Chemical Engineering and Analytical Chemistry, University of Barcelona, Martí i Franquès 1-11, 08028 Barcelona, Spain

HIGHLIGHTS

- A database consisting of 435 entries of K_d of PFASs on soils was constructed.
- K_{OC} and K_{MIN} normalized sorption coefficients of PFASs were calculated.
- Sorption on soil organic and mineral fractions increased with PFAS chain length.
- A parametric sorption model was designed to predict the K_d of PFASs in soils.
- The contribution of organic and mineral phases to PFAS sorption was quantified.

GRAPHICAL ABSTRACT

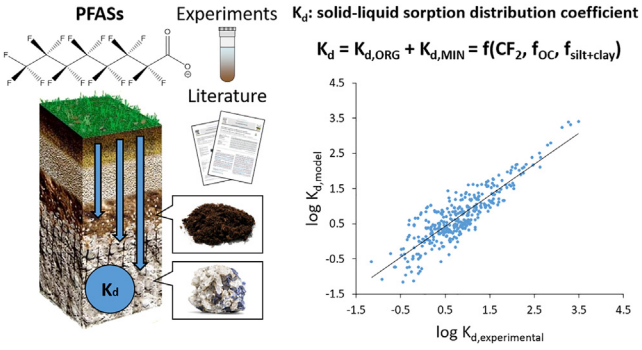

ARTICLE INFO

Article history:
Received 28 April 2021
Received in revised form 22 July 2021
Accepted 25 July 2021
Available online 30 July 2021

Editor: Shuzhen Zhang

Keywords:
PFASs
Soils
Sorption
Desorption
Modelling
K_d

ABSTRACT

A simple parametric model was developed to predict the sorption of perfluoroalkyl substances (PFASs) in soils. Initially, sorption and desorption solid-liquid distribution coefficients (K_d and $K_{d,des}$ respectively) of eight PFASs (five perfluoroalkyl carboxylates, PFCAs, and three perfluoroalkane sulfonates, PFSAs) in seven soils with organic carbon (OC) content ranging from 1.6 to 41% were quantified using batch experiments. The information obtained helped to fill the gaps in a literature-based database of K_d values of PFASs, which was lacking data on soils with high OC content. The overall dataset finally comprised 435 entries. Normalized sorption coefficients for the soil OC and mineral fraction contents (K_{OC} and K_{MIN} respectively) were deduced for each PFAS by correlating the corresponding K_d values obtained under a wide range of experimental conditions with the fraction of organic carbon (f_{OC}) of the soils. Furthermore, the sorption mechanisms in each phase were shown to depend mainly on PFAS chain length. The dependence of K_{OC} and K_{MIN} values on PFAS chain length defined the basic equations to construct the model for predicting PFAS sorption, applicable to both PFCAs and PFSAs with chain lengths ranging from 3 to 11 fluorinated carbons. The validation of the proposed model confirmed its ability to predict the K_d of PFASs based only on the soil OC and silt+clay contents and PFAS chain length. Therefore, it can be used in the first stages of a risk assessment process aiming at estimating the potential mobility of PFASs in soils after a contamination event.

Synopsis: This study develops a new parametric model to predict the sorption of perfluoroalkyl substances (PFASs) in soils.

1. Introduction

Perfluoroalkyl substances (PFASs), among them perfluoroalkyl carboxylates (PFCAs) and perfluoroalkane sulfonates (PFSAs), are anthropogenic organic pollutants with a fluorinated carbon chain attached to

* Corresponding author.
E-mail address: annarigol@ub.edu (A. Rigol).

https://doi.org/10.1016/j.scitotenv.2021.149343

a functional group. These substances have been used for more than 50 years in a variety of applications including fire-fighting foams, inks, lubricants, and oil and water repellents for the leather, paper and textile industries (Prevedouros et al., 2006). Because they are widely used, highly toxic, and can bioaccumulate and persist in the environment, PFASs have garnered considerable scientific attention in recent years (Kannan, 2011). They have been found in environmental matrices such as soil, sediment, and biological samples, as well as in rain, freshwater, seawater, and groundwater (Prevedouros et al., 2006). Specifically, they have often been detected at levels of up to a few mg kg^{-1} in contaminated soils and at levels of up to several hundred μg L^{-1} in groundwater of contaminated sites (Brusseau et al., 2020; McGuire et al., 2014). Given these high concentrations, it is important to evaluate PFAS sorption in soils in order to develop sorption prediction models and to assess their mobility in the environment.

Several soil properties have been suggested to affect PFAS sorption in soils, including organic carbon (OC), silt and clay phases, pH and status of divalent metals. Higgins and Luthy (2006) found that soil OC content was the main parameter affecting the sorption behaviour of PFASs in sediments, suggesting that most sorption occurred via hydrophobic interactions, although pH and the concentration of divalent cations might also play a role in the sorption process via electrostatic interactions. The presence of hydrophobic interactions in soils was further addressed by Milinovic et al. (2015), and the effect of salinity and pH on sorption to sediments with OC < 1% has also been evaluated elsewhere (You et al., 2010). However, even though pH and ionic strength may play a role in the sorption process on soils under controlled scenarios, these effects are minor compared to the effect of OC content. Moreover, studies exploring the sorption of PFASs on low OC soils (< 5%) have suggested that the mineral phase may have a positive influence on the sorption process (Knight et al., 2019; Martz et al., 2019). A literature review evaluating the role of soil and sediment properties in the sorption of PFASs concluded that OC alone could not satisfactorily account for the sorption of PFASs and suggested that other parameters, such as soil pH and clay content, should also be considered (Li et al., 2018). However, these conclusions were based on a data set that included mostly studies of soils or sediments with OC content <10% and very few samples of soils with higher OC content which may be representative of environmental scenarios such as meadows, forest soil layers or peat soils. In addition, the sorption pattern was deduced from the widely-evaluated PFASs perfluorosulfonic acid (PFOS) and perfluorooctanoic acid (PFOA), while only limited sorption data are available for other shorter or longer-chained PFASs in soils and sediments.

Among the models for predicting the sorption behaviour of PFASs currently in use, a mechanistic model was developed to predict the sorption of PFCAs, PFSAs, and linear alkylbenzenes in sediments with OC ranging from 0.6 to 9.7% via both electrostatic and hydrophobic interactions with the organic matter (Higgins and Luthy, 2007). The model was tested for its ability to predict the sorption parameters of PFCAs and PFSAs with 7–11 fluorinated carbons under specific experimental conditions. Moreover, Knight et al. (2019) developed a model based on OC and soil silt and clay content, able to predict the sorption of PFOA under selected experimental conditions in soils with OC content ranging from 0.1–3.5%, thus excluding organic soils. Therefore, new experimental data to derive PFAS sorption parameters in a diversity of soil types are required to improve current sorption models, making them less site-specific and covering a wide variety of PFASs, including the least commonly regulated species (especially short-chained PFASs) (Sima and Jaffé, 2021).

In this study, we aim to construct a simple and global parametric model, based on a small number of easily-measurable physicochemical properties of soil and PFASs, to predict the sorption solid-liquid distribution coefficient (K_d) of any PFCAs and PFSAs with a number of fluorinated carbon units between 3 and 11, and applicable to both mineral and organic soils. First, sorption parameters of eight PFASs in seven soils with OC ranging from 1.6 to 41% were determined to improve an overall database of K_d values of PFASs created with data from the literature. Then, a parametric model was constructed based on the relationships between normalized sorption coefficients (with respect to soil OC and mineral phase contents) and the number of fluorinated carbons.

2. Materials and methods

2.1. Reagents and standards

Milli-Q double deionized water (18.2 MΩ cm^{-1}) was obtained from a water purification system (USF PureLaB Plus, Spain). High-performance liquid chromatography-grade acetonitrile (≥99.9%), as well as extra-pure sodium azide (≥99.0%) and calcium chloride dihydrate (99%), were supplied by Merck (Germany), and ammonium acetate (96%) was supplied by Panreac (Spain). Analytical standards of perfluorobutanoic acid (PFBA) 98%, perfluorohexanoic acid (PFHxA) 97%, perfluorooctanoic acid (PFOA) 96%, perfluorononanoic acid (PFNA) 97%, perfluorododecanoic acid (PFDoA) 95%, and potassium perfluorohexane sulfonate (PFHxS) 98% were supplied by Sigma-Aldrich (Germany). Tetrabutylammonium perfluorobutane sulfonate (PFBS) 98% and tetrabutylammonium perfluorooctane sulfonate (PFOS) 95% were supplied by Fluka (Austria). Isotope-labelled sodium perfluoro-1-[1,2,3,4,-$^{13}C_4$]-octane sulfonate (MPFOS) and perfluoro-n-[1,2,3,4,-$^{13}C_4$]-octanoic acid (MPFOA), both at concentrations of 50 μg mL^{-1} in methanol, were supplied by Wellington Laboratories (Canada). Working solutions of 1000 μg mL^{-1} containing the individual PFASs were prepared in acetonitrile, whereas working solutions of MPFOS and MPFOA were prepared separately at 20 μg mL^{-1} in acetonitrile by diluting the commercial stock solutions. All solutions were stored at −18 °C in glass vials with polyethylene caps (Sigma-Aldrich, Germany).

The main physicochemical properties of all PFASs considered in this study, including those not used in our experiments but incorporated in the database for our parametric model, are summarized in Table S1. Based on the pK_a values reported in Table S1, all selected PFASs were expected to be in their anionic form under our experimental conditions. PFAS chain length in this study was referred as the total number of fluorinated carbons in the alkyl chain (CF_2) including the final $-CF_3$ moiety.

2.2. Materials and characterization

Seven field soil samples (topsoils; taken at 0–10 cm depth) with physicochemical properties varying within a wide range were selected for our PFAS sorption and desorption experiments (Table 1). The soil samples generally had an acidic pH ranging from 5.2 to 5.8 and a $CaCO_3$ content below 3%, with the exception of the DELTA2 soil, which had a slightly basic pH of 8.0 likely due to its higher $CaCO_3$ content. The OC content of the soil samples ranged from 1.6 to 41%; four samples having an OC content above 25%. More information about the soils and the physicochemical characterization procedures is provided elsewhere (Ramírez-Guinart et al., 2017).

2.3. Sorption and desorption experiments

To test the sorption behaviour of each PFAS in each soil, three grams of dried soil were placed in 80-mL polypropylene (PP) centrifuge tubes with 30 mL of 0.01 mol L^{-1} $CaCl_2$ solution containing 1 g L^{-1} of NaN_3 as a biodegradation inhibitor (OECD, 2000). The resulting suspensions were end-over-end shaken at 60 rpm for 24 h, and then known volumes of individual PFAS stock solutions were added to the suspensions. The initial spiked concentrations of each PFAS (Table S2) were selected to ensure that: i) the K_d value fell within the linear range of the sorption isotherm according to previous studies of PFAS sorption in soils performed by our research group (Milinovic et al., 2015); ii) the final sorbed concentrations were representative of concentrations that might be found in contaminated soils (Brusseau et al., 2020); iii) PFAS

Table 1
Main physicochemical properties of the soils.

Soil	Location	pH	OC (%wt)	Clay (%)	Silt (%)	Fe (mg kg^{-1})	Al (mg kg^{-1})	Mn (mg kg^{-1})	$CaCO_3$ (%wt)	CEC ($cmol_c$ kg^{-1})	DOC (mg L^{-1})	SSA (m^2 g^{-1})
ALM	Spain	5.5	1.6	10.6	35.0	1013	404	204	2.0	23.4	15	2.0
DELTA2	Spain	8.0	7.7	33.5	52.3	2966	230	330	51	87.3	39	6.5
OVI01	Spain	5.2	9.4	18.9	39.8	4515	377	390	3.0	44.3	250	1.8
UIAR	Ukraine	5.8	27	3.0	51.0	6502	1732	556	0.2	90.0	180	0.5
BRA	Belarus	5.7	32	2.0	63.0	12,358	1027	598	2.0	103	175	0.6
DUBLIN	Belarus	5.7	39	1.3	78.0	10,640	167	1443	1.6	140	290	0.6
KOM	Russia	5.7	41	1.1	78.9	19,668	481	393	0.5	114	187	0.8

concentrations in the final liquid solution were below 70 μg L^{-1}, a value also representative of concentrations found in groundwater of PFAS-impacted sites (McGuire et al., 2014); and iv) the final concentration in the liquid solution led to reliable results after their analytical determination. After being spiked with a PFAS, tubes were shaken again at 60 rpm for 24 h to ensure that the equilibrium was reached in accordance with previous kinetic studies (Li et al., 2019; Mejia-Avendaño et al., 2020; Miao et al., 2017; Wei et al., 2017; Xiang et al., 2018; Zhi and Liu, 2018). Then, tubes were centrifuged for 30 min at 4 °C and 7800 *g* (AJ2-HS, Beckman Coulter, USA) and supernatants were removed using a plastic syringe, filtered through 0.45 μm and stored in 50 mL glass vials at 4 °C until analysis. For the desorption experiments, soil residues from the sorption experiment were dried at 40 °C and then tested using the same procedure as above, but without PFAS spiking, except for PFBA and PFBS that presented, in general, very low sorption levels. Shaking desorption time was 24 h, in agreement with previous kinetic desorption experiments on soils and sediments with varying OC content (Miao et al., 2017; Zhi and Liu, 2018). In addition, preliminary studies revealed that PFAS sorption and desorption K_d values at 168 h were statistically comparable to those found at 24 h. The pH of the resulting supernatants from sorption and desorption experiments did not differ (±0.2) from the soil pH reported in Table 1.

2.4. Quality control

All sorption and desorption batch experiments were performed in duplicate. The relative standard deviation between replicates was approximately 20% in the worst scenarios. Quality control of the analyses included blank soil samples that were tested using the same procedure described in Section 2.3, but without PFAS spiking, to test whether PFASs were present in the soil samples. In addition to this, aqueous control samples at PFAS concentrations representative of the tested concentration range were assayed to quantify PFAS losses during the experimental stages of the batch test.

Results from the analyses of blank soil samples showed that no PFASs were present in the soils prior to the analysis. Regarding aqueous control samples, negligible losses for all the PFASs were observed, except for PFDoA (see Section S1). Although some authors have reported sorption of PFOA on common laboratory equipment (Lath et al., 2019), our results agree with those reported in the literature for short- and mid-chained PFASs (Ahrens et al., 2011; Milinovic et al., 2015; Campos Pereira et al., 2018). However, for the long-chained PFDoA only 40% was recovered, and the results were corrected accordingly.

2.5. PFAS analysis by LC-MS/MS

To quantify the PFAS concentration resulting from the sorption and desorption experiments, 750 μL aliquots of the supernatants were transferred into a 2-mL chromatographic vial. 10 μL of either the MPFOS or MPFOA internal standard working solution and 240 μL of acetonitrile were then added into the vial to reach a final volume of 1 mL, and the PFASs were subsequently analysed via liquid chromatography with tandem mass spectrometry (LC-MS/MS). Details of the chromatographic methods can be found in Section S1 of the Supplementary Information.

2.6. Quantification of sorption and desorption parameters

The sorption solid-liquid distribution coefficient, K_d (L kg^{-1}), was calculated as the ratio between the concentration of the target PFAS sorbed at the solid phase, C_s (ng g^{-1}), and the concentration of the target PFAS in the aqueous phase at equilibrium, C_{eq} (ng mL^{-1}):

$$K_d = \frac{C_s}{C_{eq}} \quad (1)$$

C_{eq} values were directly determined by LC-MS/MS, whereas C_s was calculated using the following equation:

$$C_s = \frac{(C_{in} - C_{eq}) \cdot V}{m} \quad (2)$$

where C_{in} (ng mL^{-1}) represents the initial concentration of PFAS in the suspension, V (mL) is the total volume of contact solution, and m (g) refers to the dry mass of soil.

The sorption percentage (%S) was calculated as follows:

$$\%S = \frac{(C_{in} - C_{eq})}{C_{in}} \cdot 100 \quad (3)$$

As with K_d (Eq. (1)), the desorption solid-liquid distribution coefficient, $K_{d,des}$ (L kg^{-1}), was calculated as follows:

$$K_{d,des} = \frac{C_{s,des}}{C_{eq,des}} \quad (4)$$

where $C_{s,des}$ (ng g^{-1}) and $C_{eq,des}$ (ng mL^{-1}) are PFAS concentrations in the solid and aqueous phases, respectively, after the desorption experiments. $C_{eq,des}$ values were directly determined by LC-MS/MS, whereas $C_{s,des}$ values were calculated as the difference between the initial PFAS concentration in the solid residue resulting from the sorption experiments ($C_{in,des}$, ng g^{-1}) and the PFAS desorbed with regard to the mass of soil, as follows:

$$C_{s,des} = C_{in,des} - \frac{C_{eq,des} \cdot V}{m} \quad (5)$$

$C_{in,des}$ depends on C_s and the amount of PFAS present in the residual volume of solution ($C_{eq} \cdot V_{res}$) that remained in the soil after the sorption experiment:

$$C_{in,des} = C_s + \frac{C_{eq} \cdot V_{res}}{m} \quad (6)$$

2.7. Construction of the PFAS K_d datasets

Two datasets including K_d values for PFASs in soils and analogous geological materials (i.e., subsoils and sediments) were constructed using our own experimental data and additional data from the literature. Our experimental dataset consisted of 56 entries, while the overall dataset (which also included our experimental data) comprised 435

entries. K_d values from the literature were only included in the data if they originated from batch experiments, given that K_d values obtained from in situ experiments have been shown to be significantly higher due to the non-equilibrium nature of natural systems (Li et al., 2018). Only studies in which a K_d value could be confidently derived (i.e., linear isotherms with constant K_d; non-linear isotherms, but with the reported K_d falling within the linear range of the isotherm; or K_d values calculated from a low initial concentration, assuming that sorption saturation was not reached) were considered. In addition, we only included data for PFCAs and PFSAs that contained from 3 to 11 fluorinated carbons. Ancillary information about the soils, such as sand, silt, clay, and OC content, was also included in both datasets.

Table S3 provides the references and information for the data used to build the overall PFAS sorption dataset. Of the 222 samples obtained from these references, 167 were soils, 171 had an OC content less than 2%, and only 10 had an OC content greater than 10%. PFOS and PFOA were the two PFASs with the highest number of entries, whereas limited data were available in the literature for other PFASs, including PFDS, PFPeA and PFHpA.

3. Results and discussion

3.1. PFAS sorption and desorption patterns in soils

The sorption K_d values for each PFAS in each of the seven soils examined are summarized in Table 2, while sorption efficiencies expressed as percentages are summarized in Table S4. Buck and co-workers suggested a unified classification of PFASs into short- and long-chained groups (Buck et al., 2011). However, due to the differences in the log K_{OW} (see Table S1) and K_d values (see Table 2) for PFHxS and PFDoA as well as PFBA and PFOA, in this study we decided to adapt the PFAS definition by grouping the PFASs into short-, mid- and long-chained. We considered PFASs with ≤5 CF_2 (PFBA, PFBS, PFPeA, and PFHxA) to be short-chained, and PFASs with 6–9 CF_2 (PFHpA, PFHxS, PFOA, PFNA, PFOS, and PFDA) and > 9 CF_2 (PFUnA, PFDS, and PFDoA) to be mid- and long-chained respectively.

Short-chained PFASs (PFBA, PFBS and PFHxA) generally had K_d values below 7 L kg^{-1}, regardless of the soil characteristics or the PFAS functional group, indicating their low sorption affinity in soils and their potentially high mobility (Gellrich et al., 2012). On the other hand, mid-chained PFASs (PFHxS, PFOA, PFOS and PFNA) had higher K_d values ranging from 2 to 295 L kg^{-1} depending on the PFAS and the soil characteristics, indicating higher sorption affinity in the soils examined and therefore lower potential mobility. Sorption in low OC soils, as exemplified by the ALM soil, was lower than in the rest of soils, and in general, K_d increased with OC content.

The sorption K_d values for the mid-chained PFHxS, PFOA and PFOS in this study were comparable to previously reported values (Higgins and Luthy, 2006; Oliver et al., 2020) and were higher than the corresponding short-chain PFASs, indicating that sorption was favoured by greater PFAS hydrophobicity. Despite having the same CF_2, PFOS had higher K_d values than PFNA, suggesting an influence of the hydrophilic functional group with a slightly higher sorption affinity of the sulfonate group than the carboxylate group. These differences between sorption affinity for PFOS and PFNA have also been described elsewhere (Enevoldsen and Juhler, 2010; Higgins and Luthy, 2006) and confirm that PFCAs have a higher mobility than PFSAs (Sepulvado et al., 2011). The long-chained PFAS, PFDoA, had the highest K_d values among the PFASs tested, with a high K_d even for the low OC ALM soil, indicating a very low mobility of these PFASs in soils.

The reversibility of the sorption process was also evaluated. The $K_{d,des}$ values obtained are reported in Table S5 and were higher than the corresponding K_d values for sorption. The hysteresis coefficient, calculated as the ratio between $K_{d,des}$ and K_d, was therefore larger than one in all cases. These results indicate the irreversibility of PFAS sorption and are in agreement with previous studies (Enevoldsen and Juhler, 2010; Miao et al., 2017). Because desorption data were scarce in the literature and only available for a few PFASs all subsequent analyses focus solely on sorption data.

Table 2
Sorption K_d values of PFASs (L kg^{-1}) in the seven soils examined. The number of CF_2 in each PFAS is shown in brackets.

Soil	PFBA (3)	PFBS (4)	PFHxA (5)	PFHxS (6)	PFOA (7)	PFNA (8)	PFOS (8)	PFDoA (11)
ALM	0.55	0.60	2.9	2.4	2.6	11	32	422
DELTA2	0.89	1.6	2.5	4.1	3.9	35	76	623
OVI01	0.33	1.4	1.2	5.4	7.1	39	110	738
UIAR	0.91	1.5	2.6	18	26	96	144	1300
BRA	1.2	3.0	5.4	17	27	117	171	2034
DUBLIN	1.7	6.8	5.1	21	38	122	295	1837
KOM	1.2	3.0	6.5	18	37	128	207	3082

3.2. Correlation of sorption and desorption parameters with soil OC

Given the importance of soil OC content for PFAS sorption and desorption parameters, especially for mid- and long-chained PFASs, the sorption K_d values reported in Table 2 were further examined for their dependence on the fraction of OC (f_{OC}), expressed as kg of OC per kg of soil. We additionally examined the relative contribution of OC and mineral binding sites to the overall sorption. Specifically, iron, aluminium and titanium oxides have all been reported to be able to interact with PFASs and to participate in PFAS sorption (Lu et al., 2016). Although a preliminary overview of our results showed that K_d values were correlated with extracted amorphous Fe content, this correlation might be attributed to the correlation between extracted Fe and soil OC ($r^2 = 0.81$) (data derived from Table 1). This conclusion agrees with previous studies which observed no correlation between K_d and Fe content in soils where OC was the primary driver of PFAS sorption (Higgins and Luthy, 2006; Miao et al., 2017).

The OC-normalized sorption coefficient (K_{OC}, L kg OC^{-1}) is defined as the ratio between K_d and the soil f_{OC} (OECD, 2000).

$$K_{OC} = \frac{K_d}{f_{OC}} \quad (7)$$

Eq. (7) considers that the sorption is driven entirely by soil OC; it may therefore overestimate K_{OC} if the soil mineral fraction plays a role in the sorption of the target compound, a situation that several authors have pointed out for PFASs in mineral soils (Knight et al., 2019; Li et al., 2018; Wang et al., 2021). Thus, a constant term has to be added in Eq. (7) referring to the sorption contribution of non-OC soil fractions, which may be attributed to the soil mineral fraction ($K_{d,MIN}$, L kg^{-1}) (Milinovic et al., 2015; Sorengard et al., 2019):

$$K_d = K_{OC}\ f_{OC} + K_{d,\ MIN} \quad (8)$$

$K_{d,MIN}$ can be quantified by extrapolating the correlation to $f_{OC} = 0$. In this scenario, sorption is driven entirely by the mineral fraction and thus $K_{d,MIN}$ could be directly considered as the normalized sorption coefficient referring to the mineral phase (K_{MIN}, L kg $mineral^{-1}$). The K_{OC} and K_{MIN} values obtained for each PFAS after applying Eq. (8) using both the overall dataset and our own are summarized in Table 3. To our knowledge, although other authors have attempted to calculate different mineral-normalized sorption coefficients (Sorengard et al., 2019; Wang et al., 2021), this is the first time that mineral-normalized sorption coefficients values have been calculated from data assembled from the literature. Significant correlations for each PFAS ($p < 0.05$) were obtained between K_d and f_{OC} for both datasets. Derived K_{MIN} values of PFASs were much lower than the respective K_{OC} values, indicating that PFASs have a higher sorption affinity to the OC sites present in the soil. The application of Eq. (8) to the overall dataset allowed us to

Table 3
Comparison of K_{OC} and K_{MIN} values for PFAS sorption derived from our experimental dataset ("own") and a larger dataset that included both our experimental data and values from the literature ("overall"). Standard errors of parameters are reported in brackets.

	Own dataset (n = 7)		Overall dataset		
	K_{OC}	K_{MIN}	K_{OC}	K_{MIN}	n
PFBA	2.3 (0.7)	0.44 (0.19)	2.9 (0.6)	0.43 (0.13)	13
PFBS	10 (3.8)	0.41 (0.11)	11 (1.5)	0.44 (0.29)	19
PFPeA	N.A.	N.A.	15 (2.4)	0.46 (0.42)	7
PFHxA	10 (3.1)	1.5 (0.83)	15 (1.8)	0.46 (0.41)	14
PFHpA	N.A.	N.A.	50 (1.3)	N.Q.	10
PFHxS	47 (5.6)	1.6 (1.5)	50 (2.2)	1.2 (0.29)	33
PFOA	94 (5.7)	N.Q.	107 (4.5)	3.3 (0.34)	182
PFOS	496 (98)	36 (27)	609 (19)	9.4 (1.8)	95
PFNA	300 (16)	11 (4.4)	324 (10)	2.0 (1.7)	20
PFDA	N.A.	N.A.	604 (221)	14 (7.7)	19
PFUnA	N.A.	N.A.	2446 (512)	25 (20)	8
PFDS	N.A.	N.A.	4605 (564)	N.Q.	5
PFDoA	5443 (1029)	208 (178)	5371 (672)	229 (152)	10

N.A.: Not analysed; N.Q.: Not quantifiable.

derive K_{OC} and K_{MIN} for PFASs not included in our experiments, such as PFPeA, PFHpA, PFDA, PFUnA, and PFDS. Since the K_d values of the overall dataset were obtained under a wide range of experimental conditions, the K_{OC} and K_{MIN} values derived were affected by the intrinsic variability of the literature data. However, K_{MIN} values derived from the overall dataset can be considered more representative than those derived from ours, as the overall dataset contained a higher number of soils with low OC.

The K_{OC} values of PFASs we obtained were lower than K_{OC} values calculated solely based on Eq. (7) reported elsewhere (Enevoldsen and Juhler, 2010; Guelfo and Higgins, 2013; McLachlan et al., 2019) but comparable to reported K_{OC} derived by considering sorption at mineral sites as well (Higgins and Luthy, 2006; Milinovic et al., 2015). Direct comparisons with previously reported K_{MIN} values were not possible. However, K_d data of PFASs are available for pure mineral phases, such as phyllosilicate minerals, which can serve as analogues for soils with $f_{OC} = 0$. The overall K_d in these materials therefore equals $K_{d,MIN}$ and, consequently, K_{MIN}. For the mid-chained PFOS and PFOA, two of the most frequently studied PFAS, the K_{MIN} values that we derived from the overall dataset were 9.4 and 3.3 respectively. These values are similar to the range of K_d values (2.6–14 L kg^{-1} for PFOS and 0.5–2.3 L kg^{-1} for PFOA) obtained on pure phyllosilicate minerals such as kaolinite and montmorillonite (Jeon et al., 2011; Johnson et al., 2007; Xiao et al., 2011), two clay minerals which are often present in soils. Furthermore, K_{MIN} values for PFOS were higher than for PFNA, in agreement with previous observations (Xiao et al., 2011). Besides, K_{MIN} values for PFASs with ≤5 CF_2 were lower than 1; this is consistent with the hypothesis that sorption of short-chained PFASs is not thermodynamically favourable under systems with low ionic strength (1–10 mM) (Xiao et al., 2011), which are the most common scenarios of the experiments used to construct the overall database.

3.3. Correlation of K_{OC} and K_{MIN} with PFAS physicochemical properties

As shown in Table S1, the hydrophobicity of the PFASs, expressed as log K_{OW}, increased linearly with each fluorinated carbon added to the alkyl chain (log K_{OW} = 0.71 (±0.08) × number of CF_2, r^2 = 0.97, p < 0.001, n = 13). Due to this strong correlation, the effect of PFAS properties on K_{OC} and K_{MIN} can reasonably be evaluated based on either the number of CF_2 or log K_{OW}. In principle, K_{OW} values better differentiate PFASs that have the same number of CF_2 but different functional groups, such as PFOS and PFNA, but log K_{OW} values vary significantly in the literature. Therefore, correlations were performed using the number of CF_2, an easily available parameter that is descriptive of PFASs.

As shown in Fig. 1, the K_{OC} and K_{MIN} values derived from both our experimental and literature-assembled datasets were logarithmically

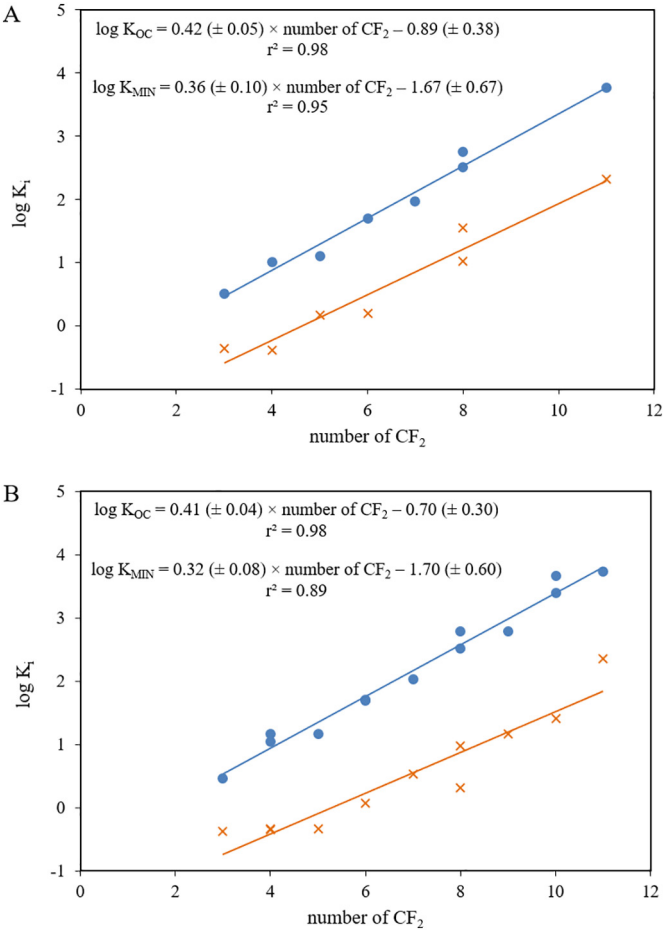

Fig. 1. Correlations between K_{OC} (blue, circle) and K_{MIN} (orange, cross) values of PFASs and the number of CF_2 of PFASs, derived from our own (A) and the overall (B) dataset.

correlated with the number of CF_2 of the PFASs reported in Table S1. The correlations were significant, and both the slope and the y-intercept were comparable between datasets. Eqs. (9) and (10) show the relationships between the number of fluorinated carbons and each of K_{OC} and K_{MIN} derived from the overall dataset:

$$\log K_{OC} = 0.41\ (\pm 0.04) \times \text{number of } CF_2 - 0.70\ (\pm 0.30) \quad (r^2 = 0.98;\ p < 0.001) \tag{9}$$

$$\log K_{MIN} = 0.32\ (\pm 0.08) \times \text{number of } CF_2 - 1.70\ (\pm 0.60) \quad (r^2 = 0.89;\ p < 0.001) \tag{10}$$

The high quality of these correlations allowed us to derive predicted K_{OC} and K_{MIN} values for PFASs for which only the number of CF_2 units were available. In agreement with previous findings (Milinovic et al., 2015), K_{OC} values increased with higher PFAS hydrophobicity, which strongly suggested that sorption to OC was mainly driven by hydrophobic interactions. Humic substances, which are the main organic compounds present in the soil organic phase, often possess hydrophilic moieties that can also interact with PFASs through mechanisms such as hydrogen bonding or divalent cation bridging (Du et al., 2014). However, experiments testing the sorption of PFASs on humic acids extracted from soils have shown that these hydrophilic contributions are not predominant, thus confirming that hydrophobic interactions are the main sorption mechanism (Xiang et al., 2018; Zhao et al., 2014).

K_{MIN} values also increased with increasing PFAS chain length, a finding that is comparable to the K_d increase reported for the C_7–C_{10} PFAS

series on kaolinite clay (Xiao et al., 2011). The interaction between the negatively charged kaolinite surface and the negatively charged PFAS could be explained by the presence of divalent cations either acting as an intermediate bridge in electrostatic interactions (Du et al., 2014), which may explain the positive effects of the presence of calcium on the K_d of PFASs (Higgins and Luthy, 2006), or inhibiting the negative repulsions within the electrical double layer of the mineral surface (Xiao et al., 2011). Moreover, recent computational studies have identified the hydrophobic patches of montmorillonite clay as the primary adsorption domains and the stabilization of adsorption enthalpy in the presence of cations (Willemsen and Bourg, 2021). Nevertheless, further mechanistic insights between negatively charged PFASs and different clay minerals are still required. Overall, these results suggest that both sorption of the PFASs in the mineral and organic phases of the soil become more favourable as the PFAS chain length increases. However, the ratio between K_{OC} and K_{MIN} values also increased with increasing PFAS chain length, indicating that long-chained PFASs have a higher affinity for the organic phases than mid- and short-chained PFASs.

3.4. Development and validation of a PFAS sorption model in soils

To develop a parametric model to predict the sorption of PFCAs and PFSAs in soils based only on the number of CF_2 of PFASs and on a few physicochemical properties of the soil, we used the correlations presented in Eqs. (9) and (10) as descriptors of the sorption on the OC and mineral pool sites respectively. Based on a multiple regression analysis, Li et al. concluded that soil OC, clay content, and pH all have a significant effect on the K_d of PFASs (Li et al., 2018). Similarly, Knight et al. found that OC and the mineral silt and clay fractions contributed significantly to the sorption of PFOA in a large number of mineral soils (Knight et al., 2019). The silt and clay fractions have also been reported to have a positive effect on the K_d of PFOS, PFOA and PFHxS in sediments (Oliver et al., 2020), and a study of PFOA sorption on various soil size fractions confirmed that K_d decreases along the sequence: clay > fine silt > coarse silt > fine sand > coarse sand (Xiang et al., 2018). Indeed, Wang and co-workers derived silt+clay normalized sorption coefficients using a three-compartment distribution model to account for the contribution of the mineral fraction to the overall K_d (Wang et al., 2021).

Preliminary attempts to model the K_d values of PFASs in soils based only on CF_2 and OC led to an underestimation of K_d values in mineral soils, thus highlighting that the mineral contribution needed to be considered in the modelling. Therefore, the K_d of PFASs was further modelled from a separate contribution of the organic and mineral phases ($K_{d,ORG}$ and $K_{d,MIN}$ respectively), regardless of the f_{OC} value:

$$K_d = K_{OC}\ f_{OC} + K_{MIN}\ f_{MIN} \quad (11)$$

where f_{MIN} is the mineral fraction, expressed as kg of mineral per kg of soil. According to the above discussion, the mineral phases mainly responsible for PFAS sorption are silt and clay. Then, f_{MIN} should be limited to the silt+clay fraction, f_{S+C}, expressed as kg of silt+clay per kg of soil, and the K_{MIN} values reported in Table 3 could be considered as silt+clay normalized sorption coefficients (L kg silt+clay^{-1}), leading to the following model based on OC, CF_2 and silt+clay content:

$$K_d = K_{OC}\ f_{OC} + K_{MIN}\ f_{S+C} = 10^{(0.41\ \times\ \text{number of } CF_2\ -\ 0.70)}\ f_{OC} + 10^{(0.32\ \times\ \text{number of } CF_2\ -\ 1.70)}\ f_{S+C} \quad (12)$$

We tested the predictive ability of this model using only the entries from our datasets that contained data for both soil OC and textural fractions. The predictive accuracy for the model was quite satisfactory both for our experimental data and for the overall dataset (see Fig. 2a and b). The model's RMSE and RPD values (calculated according to Section S2) indicated that its quality was acceptable. The model's predictive ability increased if the K_{OC} and K_{MIN} values for each PFAS, reported in Table 3, were used in the model rather than the K_{OC} and K_{MIN} values predicted from the correlations with the number of CF_2 ($\log K_{d,model} = 0.92\ (\pm 0.05) \times \log K_{d,exp}$, $r^2 = 0.78$, $p < 0.001$, $n = 353$). In that case, RMSE and RPD values were 0.37 and 1.94, respectively. However, this model cannot be applied to PFASs for which no K_{OC} and K_{MIN} data are available. Although the inclusion of other soil properties (e.g., the status of divalent metal ions, pH, or metal oxide content) could be examined to further improve the established prediction model, this would also increase the model's complexity without enhancing its range of applications. Nevertheless, according to the RPD values derived from the predictions of the overall dataset, we warn against the use of the model for attempting to derive very accurate K_d values of PFASs in soils. In Fig. 2b some scattering of the data is observed for scenarios with low sorption, likely attributable to the weak interaction between PFAS and the solid phase, in addition to the intrinsic variability due to the use of literature-assembled data. The model, instead, may be capable of predicting approximate K_d values for categorizing scenarios with very low (K_d < 10 L kg^{-1}), medium (K_d of 10–1000 L kg^{-1}), and high (K_d > 1000 L kg^{-1}) sorption. According to the associated risk, intervention actions and/or more accurate site-specific K_d values could be deduced from further in-situ studies. Besides, it is unclear at present how the model would behave with regard to the prediction of PFAS species other than PFCAs and PFSAs with a number of fluorinated carbons between 3 and 11.

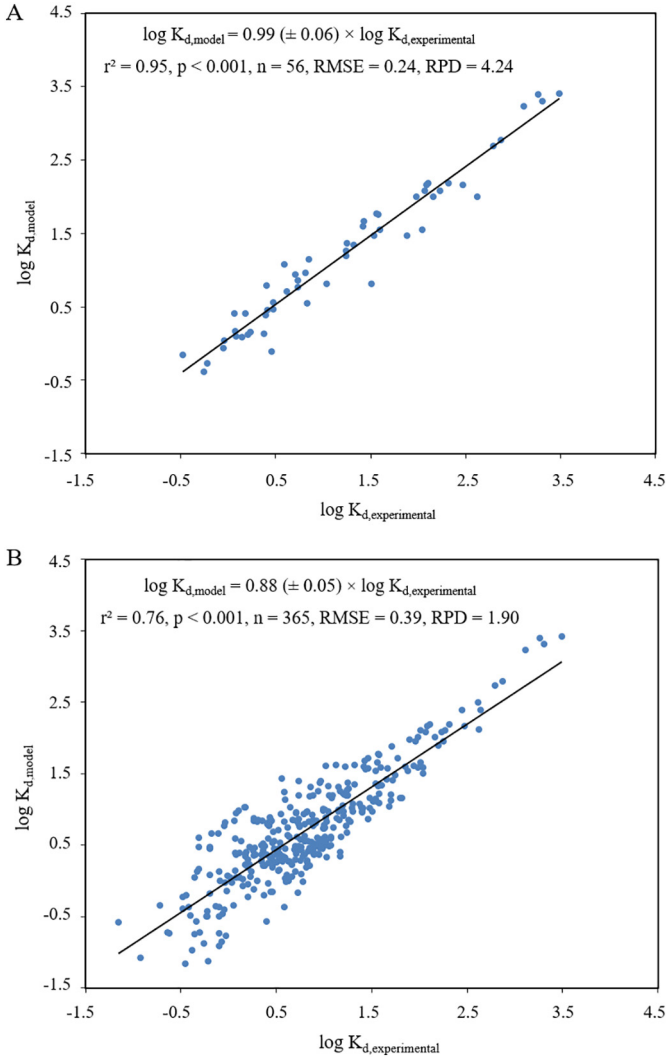

Fig. 2. Predictive ability of the K_d model of PFASs based on OC, silt+clay and CF_2 for (A) our own experimental dataset and (B) the overall dataset.

Table 4
Contribution of the mineral sorption sites to the overall K_d for different OC-content soils and PFASs.

	PFBS			PFOA			PFOS			PFDoA		
Soil group (% OC)	n	K_d	% $K_{d,MIN}$	n	K_d	% $K_{d,MIN}$	n	K_d	% $K_{d,MIN}$	n	K_d	% $K_{d,MIN}$
<2	8	0.07–0.8	20–95	119	0.5–15	3–93	44	1.8–48	3–90	2	156–422	12–13
2–10	4	0.8–2.4	18–37	28	0.9–20	3–43	23	14–110	3–37	3	407–738	3–7
>10	4	1.5–6.8	≤3	6	27–41	<3	6	144–295	<3	4	1300–3082	<3

For the external validation of our proposed model, we used the Kennard and Stone method (Kennard and Stone, 1969) to select two-thirds of the data from the overall dataset as a calibration set for training the model, while the remaining one-third of the data was used as a representative validation set. K_{OC} and K_{MIN} values were first recalculated for the calibration set data according to Eq. (8), and the correlations between each parameter and CF_2 were similarly recalculated. Both the resulting slopes and intercepts of the K_{OC} and K_{MIN} correlations with CF_2 were statistically comparable to Eqs. (9) and (10), demonstrating that the model obtained from the calibration data was equivalent to the model obtained from the full data set. We then used the model from the calibration data to predict K_d for the validation data set, leading to an accurate prediction ($\log K_{d,model} = 0.9\ (\pm 0.1) \times \log K_{d,exp}$; $r^2 = 0.76$, $p < 0.001$, $n = 121$, RMSE = 0.40, RPD = 1.88).

Although OC sites have a higher affinity for PFAS sorption than silt+clay sites (that is, K_{OC} is higher than K_{MIN}), the relative amount of OC and mineral sites also influences the total K_d of a given PFAS in a given soil. Thus, mineral sites may govern PFAS sorption in mineral soils with low OC, especially in the case of short and mid-chained PFASs. We therefore used our well-established prediction model to quantify the actual distribution of PFASs among OC and silt+clay sites. The proportional contribution of mineral sites, which we quantified as the percentage of $K_{d,MIN}$ with respect to the overall K_d (% $K_{d,MIN}$), was calculated using the K_d values predicted from the overall dataset. We specifically evaluated % $K_{d,MIN}$ for PFBS, PFOA, PFOS and PFDoA, which served as representatives of short-, mid-, and long-chained PFASs. Results were grouped by soil classes defined by their OC content, as shown in Table 4. Sorption at OC sites was predominant (% $K_{d,MIN} \leq 3$) for all the PFASs in soils with OC > 10%. In soils with a lower OC content, especially <2%, the contribution of mineral sites (% $K_{d,MIN}$) varied significantly with the soil and PFAS properties, as the % $K_{d,MIN}$ values depended on the silt+clay content (higher % $K_{d,MIN}$ for higher silt+clay content). Thus, % $K_{d,MIN}$ increased with the silt+clay content, especially for the soils with OC < 2% and the short-chained PFASs. Despite this relatively higher PFAS affinity for mineral sites in low OC soils, we note that low OC soils had generally low overall K_d values of PFASs, indicating that in these soils PFAS contamination might present a higher environmental risk.

4. Conclusions

The results of the present study confirm that the overall sorption behaviour of PFASs in soils of varying OC content can be estimated by modelling the relative sorption at OC and mineral sites. Specifically, the model presented is able to predict, with acceptable accuracy, scenarios from very low to high sorption of target PFCAs and PFSAs (with a total number of fluorinated carbons ranging from 3 to 11), based on only a few physicochemical properties of the soil (OC and silt+clay content) and the number of fluorinated carbons of the target PFAS. This information may be relevant for an early evaluation of contamination events. Although soil OC content is the main parameter governing PFAS sorption, the relative contribution of the sorption at mineral sites can be significant when short-chained PFASs are sorbed in soils with low OC and high silt+clay content. However, the associated K_d of PFASs for these scenarios are very low, and therefore a high related PFAS mobility is expected.

Funding sources

This work was supported by the Ministerio de Ciencia e Innovación de España (CTM2017-87107-R) and the Generalitat de Catalunya (2017 SGR 907).

CRediT authorship contribution statement

Joel Fabregat-Palau: Conceptualization, Investigation, Formal analysis, Data curation, Writing – original draft. **Miquel Vidal:** Conceptualization, Methodology, Investigation, Supervision, Formal analysis, Writing – review & editing. **Anna Rigol:** Conceptualization, Methodology, Investigation, Supervision, Formal analysis, Writing – review & editing.

Declaration of competing interest

The authors declare that they have no known competing financial interests or personal relationships that could have appeared to influence the work reported in this paper.

Acknowledgements

The authors thank Nina Carreras and Eleana Conceição for their contribution as part of their bachelor's degree final project.

Appendix A. Supplementary data

Supplementary data to this article can be found online at https://doi.org/10.1016/j.scitotenv.2021.149343.

References

Ahrens, L., Yeung, L.W.Y., Taniyasu, S., Lam, P.K.S., Yamashita, N., 2011. Partitioning of perfluorooctanoate (PFOA), perfluorooctane sulfonate (PFOS) and perfluorooctane sulfonamide (PFOSA) between water and sediment. Chemosphere 85 (5), 731–737. https://doi.org/10.1016/j.chemosphere.2011.06.046.

Brusseau, M.L., Anderson, R.H., Guo, B., 2020. PFAS concentrations in soils: background levels versus contaminated sites. Sci. Total Environ. 740, 140017. https://doi.org/10.1016/j.scitotenv.2020.140017.

Buck, R.C., Franklin, J., Berger, U., Conder, J.M., Cousins, I.T., de Voogt, P., Jensen, A.A., Kannan, K., Mabury, S.A., van Leeuwen, S.P.J., 2011. Perfluoroalkyl and polyfluoroalkyl substances in the environment: terminology, classification, and origins. Integr. Environ. Assess. 7 (4), 513–541. https://doi.org/10.1002/ieam.258.

Campos Pereira, H., Ullberg, M., Kleja, D.B., Gustafsson, J.P., Ahrens, L., 2018. Sorption of perfluoroalkyl substances (PFASs) to an organic soil horizon – effect of cation composition and pH. Chemosphere 207, 183–191. https://doi.org/10.1016/j.chemosphere.2018.05.012.

Du, Z., Deng, S., Bei, Y., Huang, Q., Wang, B., 2014. Adsorption behavior and mechanism of perfluorinated compounds on various adsorbents — a review. J. Hazard. Mater. 274, 443–454. https://doi.org/10.1016/j.jhazmat.2014.04.038.

Enevoldsen, R., Juhler, R.K., 2010. Perfluorinated compounds (PFCs) in groundwater and aqueous soil extracts: using inline SPE-LC-MS/MS for screening and sorption characterisation of perfluorooctane sulphonate and related compounds. Anal. Bioanal. Chem. 398 (3), 1161–1172. https://doi.org/10.1007/s00216-010-4066-0.

Gellrich, V., Stahl, T., Knepper, T.P., 2012. Behavior of perfluorinated compounds in soils during leaching experiments. Chemosphere 87 (9), 1052–1056. https://doi.org/10.1016/j.chemosphere.2012.02.011.

Guelfo, J.L., Higgins, C.P., 2013. Subsurface transport potential of perfluoroalkyl acids at aqueous film-forming foam (AFFF)-impacted sites. Environ. Sci. Technol. 47 (9), 4164–4171. https://doi.org/10.1021/es3048043.

Higgins, C.P., Luthy, R.G., 2006. Sorption of perfluorinated surfactants on sediments. Environ. Sci. Technol. 40, 7251–7256. https://doi.org/10.1021/es061000n.

Higgins, C.P., Luthy, R.G., 2007. Modeling sorption of anionic surfactants onto sediment materials: an a priori approach for perfluoroalkyl surfactants and linear alkylbenzene sulfonates. Environ. Sci. Technol. 41 (9), 3254–3261. https://doi.org/10.1021/es062449j.

Jeon, J., Kannan, K., Lim, B.J., An, K.G., Kim, S.D., 2011. Effects of salinity and organic matter on the partitioning of perfluoroalkyl acid (PFAs) to clay particles. J. Environ. Monitor. 13 (6), 1803–1810. https://doi.org/10.1039/c0em00791a.

Johnson, R.L., Anschutz, A.J., Smolen, J.M., Simcik, M.F., Lee Penn, R., 2007. The adsorption of perfluorooctane sulfonate onto sand, clay, and iron oxide surfaces. J. Chem. Eng. Data 52 (4), 1165–1170. https://doi.org/10.1021/je060285g.

Kannan, K., 2011. Perfluoroalkyl and polyfluoroalkyl substances: current and future perspectives. Environ. Chem. 8, 333–338. https://doi.org/10.1071/EN11053.

Kennard, R.W., Stone, L.A., 1969. Computer aided design of experiments. Technometrics 11 (1), 137–148. https://doi.org/10.1080/00401706.1969.10490666.

Knight, E.R., Janik, L.J., Navarro, D.A., Kookana, R.S., McLaughlin, M.J., 2019. Predicting partitioning of radiolabelled 14C-PFOA in a range of soils using diffuse reflectance infrared spectroscopy. Sci. Total Environ. 686, 505–513. https://doi.org/10.1016/j.scitotenv.2019.05.339.

Lath, S., Knight, E.R., Navarro, D.A., Kookana, R.S., McLaughlin, M.J., 2019. Sorption of PFOA onto different laboratory materials: filter membranes and centrifuge tubes. Chemosphere 222, 671–678. https://doi.org/10.1016/j.chemosphere.2019.01.096.

Li, Y., Oliver, D.P., Kookana, R.S., 2018. A critical analysis of published data to discern the role of soil and sediment properties in determining sorption of per and polyfluoroalkyl substances (PFASs). Sci. Total Environ. 628–629, 110–120. https://doi.org/10.1016/j.scitotenv.2018.01.167.

Li, F., Fang, X., Zhou, Z., Liao, X., Zou, J., Yuan, B., Sun, W., 2019. Adsorption of perfluorinated acids onto soils: kinetics, isotherms, and influences of soil properties. Sci. Total Environ. 649, 504–514. https://doi.org/10.1016/j.scitotenv.2018.08.209.

Lu, X., Deng, S., Wang, B., Huang, J., Wang, Y., Yu, G., 2016. Adsorption behavior and mechanism of perfluorooctane sulfonate on nanosized inorganic oxides. J. Colloid Interf. Sci. 474, 199–205. https://doi.org/10.1016/j.jcis.2016.04.032.

Martz, M., Heil, J., Marschner, B., Stumpe, B., 2019. Effects of soil organic carbon (SOC) content and accessibility in subsoils on the sorption processes of the model pollutants nonylphenol (4-n-NP) and perfluorooctanoic acid (PFOA). Sci. Total Environ. 672, 162–173. https://doi.org/10.1016/j.scitotenv.2019.03.369.

McGuire, M.E., Schaefer, C., Richards, T., Backe, W.J., Field, J.A., Houtz, E., Sedlak, D.L., Guelfo, J.L., Wunsch, A., Higgins, C.P., 2014. Evidence of remediation-induced alteration of subsurface poly- and perfluoroalkyl substance distribution at a former firefighter training area. Environ. Sci. Technol. 48 (12), 6644–6652. https://doi.org/10.1021/es5006187.

McLachlan, M.S., Felizeter, S., Klein, M., Kotthoff, M., de Voogt, P., 2019. Fate of a perfluoroalkyl acid mixture in an agricultural soil studied in lysimeters. Chemosphere 223, 180–187. https://doi.org/10.1016/j.chemosphere.2019.02.012.

Mejia-Avendaño, S., Zhi, Y., Yan, B., Liu, J., 2020. Sorption of polyfluoroalkyl surfactants on surface soils: effect of molecular structures, soil properties, and solution chemistry. Environ. Sci. Technol. 54 (3), 1513–1521. https://doi.org/10.1021/acs.est.9b04989.

Miao, Y., Guo, X., Peng, D., Fan, T., Yang, C., 2017. Rates and equilibria of perfluorooctanoate (PFOA) sorption on soils from different regions of China. Ecotoxicol. Environ. Saf. 139, 102–108. https://doi.org/10.1016/j.ecoenv.2017.01.022.

Milinovic, J., Lacorte, S., Vidal, M., Rigol, A., 2015. Sorption behaviour of perfluoroalkyl substances in soils. Sci. Total Environ. 511, 63–71. https://doi.org/10.1016/j.scitotenv.2014.12.017.

OECD, 2000. OECD 106 Adsorption - Desorption Using a Batch Equilibrium Method. OECD Guideline for the Testing of Chemicals. https://doi.org/10.1787/9789264069602-en.

Oliver, D.P., Navarro, D.A., Baldock, J., Simpson, S.L., Kookana, R.S., 2020. Sorption behaviour of per- and polyfluoroalkyl substances (PFASs) as affected by the properties of coastal estuarine sediments. Sci. Total Environ. 720, 137263. https://doi.org/10.1016/j.scitotenv.2020.137263.

Prevedouros, K., Cousins, I.T., Buck, R.C., Korzeniowski, S.H., 2006. Sources, fate and transport of perfluorocarboxylates. Environ. Sci. Technol. 40 (1), 32–44. https://doi.org/10.1021/es0512475.

Ramírez-Guinart, O., Salaberria, A., Vidal, M., Rigol, A., 2017. Assessing soil properties governing radiosamarium sorption in soils: can trivalent lanthanides and actinides be considered as analogues? Geoderma 290, 33–39. https://doi.org/10.1016/j.geoderma.2016.12.010.

Sepulvado, J.G., Blaine, A.C., Hundal, L.S., Higgins, C.P., 2011. Occurrence and fate of perfluorochemicals in soil following the land application of municipal biosolids. Environ. Sci. Technol. 45 (19), 8106–8112. https://doi.org/10.1021/es103903d.

Sima, M.W., Jaffé, P.R., 2021. A critical review of modeling poly- and perfluoroalkyl substances (PFAS) in the soil-water environment. Sci. Total Environ. 757, 143793. https://doi.org/10.1016/j.scitotenv.2020.143793.

Sorengard, M., Berggren, D., Ahrens, L., 2019. Stabilization of per- and polyfluoroalkyl substances (PFASs) with colloidal activated carbon (PlumeStop ®) as a function of soil clay and organic matter content. J. Environ. Manag. 249, 109345. https://doi.org/10.1016/j.jenvman.2019.109345.

Wang, Y., Khan, N., Huang, D., Carroll, K.C., Brusseau, M.L., 2021. Transport of PFOS in aquifer sediment: transport behavior and a distributed-sorption model. Sci. Total Environ. 779, 146444. https://doi.org/10.1016/j.scitotenv.2021.146444.

Wei, C., Song, X., Wang, Q., Hu, Z., 2017. Sorption kinetics, isotherms and mechanisms of PFOS on soils with different physicochemical properties. Ecotoxicol. Environ. Saf. 142, 40–50. https://doi.org/10.1016/j.ecoenv.2017.03.040.

Willemsen, J.A.R., Bourg, I.C., 2021. Molecular dynamics simulation of the adsorption of per- and polyfluoroalkyl substances (PFASs) on smectite clay. J. Colloid Interface Sci. 585, 337–346. https://doi.org/10.1016/j.jcis.2020.11.071.

Xiang, L., Xiao, T., Yu, P.F., Zhao, H.M., Mo, C.H., Li, Y.W., Li, H., Cai, Q.Y., Zhou, D.M., Wong, M.H., 2018. Mechanism and implication of the sorption of perfluorooctanoic acid by varying soil size fractions. J. Agric. Food Chem. 66 (44), 11569–11579. https://doi.org/10.1021/acs.jafc.8b03492.

Xiao, F., Zhang, X., Penn, L., Gulliver, J.S., Simcik, M.F., 2011. Effects of monovalent cations on the competitive adsorption of perfluoroalkyl acids by kaolinite: experimental studies and modeling. Environ. Sci. Technol. 45 (23), 10028–10035. https://doi.org/10.1021/es202524y.

You, C., Jia, C., Pan, G., 2010. Effect of salinity and sediment characteristics on the sorption and desorption of perfluorooctane sulfonate at sediment-water interface. Environ. Pollut. 158 (5), 1343–1347. https://doi.org/10.1016/j.envpol.2010.01.009.

Zhao, L., Zhang, Y., Fang, S., Zhu, L., Liu, Z., 2014. Comparative sorption and desorption behaviors of PFHxS and PFOS on sequentially extracted humic substances. J. Environ. Sci. 26 (12), 2517–2525. https://doi.org/10.1016/j.jes.2014.04.009.

Zhi, Y., Liu, J., 2018. Sorption and desorption of anionic, cationic and zwitterionic polyfluoroalkyl substances by soil organic matter and pyrogenic carbonaceous materials. Chem. Eng. J. 346, 682–691. https://doi.org/10.1016/j.cej.2018.04.042.